AIChE

When Does a Vessel Become a Pipe?

Haroun Mahgerefteh, Navid Jalali, and Maria Isabel Fernandez
Dept. of Chemical Engineering, University College London, London WC1E 7JE, U.K.

DOI 10.1002/aic.12541
Published online February 28, 2011 in Wiley Online Library (wileyonlinelibrary.com).

The conditions under which the transient outflow from a punctured pipeline may be approximated as that emanating from a vessel using a simplified analytically based vessel blowdown model (VBM) is investigated in this article. The above addresses the fundamental drawback of long computational run times associated with the numerically based techniques used for simulating pipeline puncture failures. The efficacy of the VBM is tested by comparison of its predictions against simulation data obtained using a validated rigorous but computationally demanding numerical technique based on the method of characteristics. The results show that the accuracy of the VBM increases with decreasing puncture/pipe diameter ratio, line pressure, and increasing pipeline length. Surprisingly, the VBM produces more accurate predictions for two-phase mixtures when compared with permanent gases. This is found to be a consequence of the better applicability of the isothermal bulk fluid decompression assumption within the pipeline in the case of two-phase mixtures. © 2011 American Institute of Chemical Engineers *AIChE J,* 57: 3305–3314, 2011
Keywords: safety, environmental engineering, fluid mechanics, computational fluid dynamics, mathematical modeling

Introduction

Pressurized pipelines are extensively used for transporting significant quantities of hydrocarbons across the globe. Given the highly flammable nature of the inventories conveyed coupled with the high pressures involved (typically above 100 bar) pipeline failures have on many occasions led to catastrophic consequences both in terms of fatalities and environmental damage.[1] Even in the United States, which has one of the most stringent pipeline safety regulations in the developed world, data published by the Office of Pipeline Safety (2009) indicates 5600 serious pipeline failure incidents between 1990 and 2009.[2] These have resulted in 365 fatalities and over $4,382 m damage to property.

Given the above, an essential part of the safety assessment for pressurized pipelines involves the prediction of the discharge rate and its variation with time in the event of pipeline failure. Such data is central to assessing all the consequences associated with pipeline failure including, fire, explosion, atmospheric dispersion, and emergency planning. Even the pipeline's susceptibility to catastrophic long propagating fractures following a puncture is governed by the rate of loss of the inventory.[3]

The safety of pressurized pipelines (see for example[4]) has recently attracted renewed attention given that such mode of transportation is now widely accepted as the most practical way of conveying the captured CO_2 from fossil fuel power plants for subsequent sequestration. At concentrations greater than 7% v/v, the gas is likely to be instantly fatal.[5] As such, the likelihood of a CO_2 pipeline failure is an important issue.

Given the above, the development of accurate, robust, and computationally efficient mathematical models for predicting discharge rates following pipeline failure has been the focus of considerable attention (see for example[6–12]).

The success of these models invariably depends on their ability to capture all the important processes and their complex interactions taking place during depressurization. These include expansion wave propagation, phase- and flow-dependent heat transfer, friction effects, and the use of

Correspondence concerning this article should be addressed to H. Mahgerefteh at h.mahgerefteh@ucl.ac.uk.

reliable equations of state for producing the required phase equilibrium data. A review of the efficacies of these various models may be found in previous publications (see for example[6,12]), and hence, only a brief account is given here.

The starting point for all robust pipeline outflow models is the formulation of the mass, momentum, and energy conservation equations. In the main, two different approaches are adopted.

The more rigorous models (see for example[13–15]) account for thermal and mechanical nonequilibrium effects such as phase slip between the constituent phases during rapid depressurization. Such so-called two-fluid models were initially developed in the early 70's in the nuclear industry for the analysis of steam/water flow in the core of a nuclear reactor.[16] The dynamic two-fluid model, OLGA[13] for example, has been specifically developed for prediction of steady-state pressure drop, liquid hold-up, and flow regime transitions for hydrocarbon pipelines. However, very limited progress has been made in extending OLGA to the highly unsteady-state flows involving the rupture of hydrocarbon pipelines.[17] This is due to OLGA's reliance on the availability of empirical data such as the transition between the various flow regimes, bubble nucleation and evolution dynamics, and the numerical simulation's instability problems. Also, there is little information regarding the formulation of the choking conditions at the rupture plane, critical for the correct modeling of such highly transient flows. Finally, the fact that separate conservations are required for each constituent phase means that such two-fluid models are in principle extremely computationally demanding. The two-fluid model PLAC[14] on the other hand sharing similar underlying theory to OLGA has been shown[12] to produce poor agreement with release data obtained based on the rupture of real hydrocarbon pipelines.

Chen et al.[11,12] partly overcame such problems by developing a marginally stable model based on extending the Geurst's variation principle.[18] The model accounts for phase slip but ignores nonequilibrium thermal effects. Based on comparison with real pipeline rupture data,[19] the authors showed that nonequilibrium effects are only important in the case of short pipelines. For long pipelines ($>$100 m), both phase slip and interphase thermal stratification may be ignored, hence the far simpler and more robust homogenous equilibrium model (HEM) becomes applicable.

The coupling of the conservation equations with the appropriate correlations for predicting the fluid thermophysical and hydrodynamic properties during the pipeline depressurization results in a set of hyperbolic equations. Given that these can only be solved using a numerical technique, and their resolution can often be exceptionally computationally demanding. This is especially so for punctures; the most common type of pipeline failure.[7]

For example, the computational run time for the simulation of the complete depressurization of a 100 km, 0.8-m pipeline conveying natural gas at 100 bar following a 15-cm puncture is 18 h using a relatively high-specification (e.g., 2.66 GHz, 3.0-GB RAM) personal computer. This is despite significant progress in the development of fast solution algorithms such as nested grid systems,[6,7] interpolation techniques,[10] and the more fundamental approaches involving the formulation of the conservation equations using different combinations of primitive variables.[9]

Paradoxically, long computational run times in the case of puncture failure simulation of pressurized vessels are of no concern. This is because during such failures, in contrast to pipelines, there is little relative flow between the discharging fluid and containment wall thus resulting in negligible pressure drop within the bulk fluid. Thus, the formulation of outflow from a punctured vessel reduces to a set of equations that can be solved analytically.[20]

The tantalizing question is if and under what conditions the transient outflow from a punctured pipeline can be approximated as that emanating from a vessel.

In an attempt to address the long computational workloads associated with simulating pipeline ruptures, a number of authors have proposed simplistic pipeline models based on steady-state flow assumptions for which analytical solutions are obtainable. Norris,[21,22] for example, proposes a 'unified outflow model' for vessels and pipelines. Apart from the steady-state flow assumption, the model ignores wave dynamics and pipe/wall heat-transfer effects. The relevant fluid properties and phases are determined based on quadratic equations obtained by curve fitting of a series of either isothermal or isentropic flashes carried out over a range of pressures using an equation-of-state. The model's validation is confined to the experiments using cylindrical gas bottles discharging air, CO_2, carbonated water, methane, and hydrocarbon gas mixtures through a narrow diameter (ca., 1 cm i.d) 300-m long coil tubing approximated as a pipeline. A series of discharge diameters at the end of the tube including full bore are used.

Given that the experimental arrangement essentially involves the steady-state depressurization of a vessel discharging through a long nozzle, the observed reasonably good agreement of the model's predictions in comparison to the experimental measurements is not surprising. This finding is of little value in establishing the range of applicability of the proposed model in simulating rupture of real pipelines. Certainly, the model is inappropriate for simulating full bore rupture, where the impact of the significant pressure drop at the rupture plane and the subsequent wave propagation toward the intact end of the pipeline can not be ignored.[6] Finally, given the narrow tube diameter used, wall effects[23] are expected to play an important role in affecting the discharge rate.

This study investigates the range of applicability of a simplistic vessel blowdown model (VBM) for predicting the transient discharge rates following pressurized pipeline punctures. The model is aimed at addressing the long computational run times synonymous with simulating such failures. Its efficacy is determined by comparison of its predictions against those obtained using a previously validated robust but computationally demanding numerical model[6,10] based on the solution of the conservation equations using the method of characteristics.[24] The investigations are performed for various puncture/pipeline diameter ratios, initial line pressures, pipe lengths, and different fluid inventories including permanent gas and two-phase mixtures. Pressurized liquid pipelines are of no concern in this study due to the almost instantaneous depressurization to ambient conditions on failure.

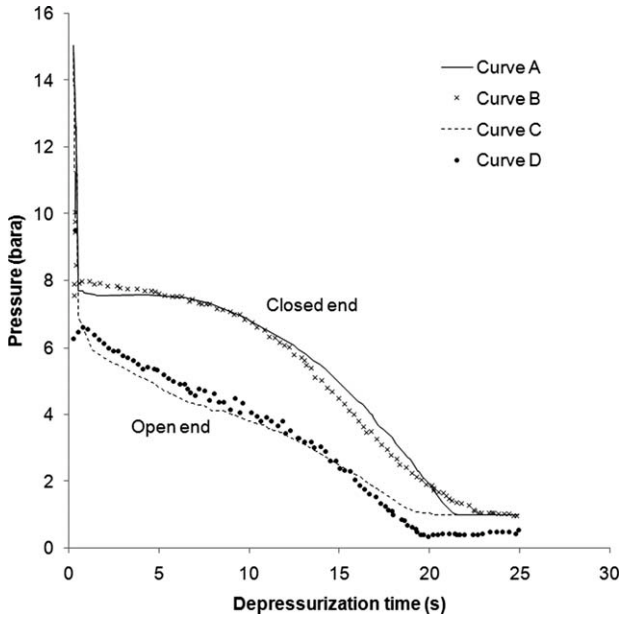

Figure 1. Pressure–time profiles at closed and open ends for the Isle of Grain full bore rupture P40 Test (LPG).

Curve A: field data (closed end); Curve B: PipeTech predictions (closed end); Curve C: field data (open end); Curve D: PipeTech predictions (open end).

Theory

Pipeline rupture model

Full details of the numerically based pipeline rupture model, translated into the computer program PipeTech[25] used in this study for testing the efficacy of the VBM are given elsewhere[6,10] and hence only a brief account is given here.

Much the same as Chen et al.'s[12] pipeline rupture model, PipeTech is based on the homogeneous flow assumption. However, a number of fundamentally important improvements have been made to reduce the computational run time, increase simulation accuracy, and improve flexibility in terms of application to real pipeline systems.

For example, in PipeTech, the conservation equations are posed in terms of the dependent variables pressure, P, specific enthalpy, h_e, and flow velocity, u,[9] as opposed to P, density, ρ, and u. This approach, coupled with the development of a pressure/enthalpy interpolation grid[10] serving as a look up table significantly, reduces the number of flash calculations and hence the computational workload. Also, PipeTech uses a phase-dependent heat-transfer coefficient resulting in a better prediction of the fluid temperature especially during the latter stages of depressurization where fluid/wall heat-transfer effects become important. Finally, the use of specified time intervals method as opposed to the wave tracing method[24] for solving the conservation equations (see later) allows the placing of the appropriate boundary conditions for simulating emergency shutdown valve closure with relative ease.[26]

Based on the HEM assumption, the conservation equations for one-dimensional (1-D) flow in a pipeline expressed in terms of pressure, specific enthalpy, and flow velocity as dependent variables are given by[7]:

$$[\rho T + \psi]\frac{dP}{dt} - \rho\psi\frac{dh_e}{dt} + \rho^2 a^2 T\frac{\partial u}{\partial x} = 0 \tag{1}$$

$$\rho\frac{du}{dt} = -\frac{\partial P}{\partial x} - \rho g\sin\theta + \beta_x \tag{2}$$

$$\rho\frac{dh_e}{dt} - \frac{dP}{dt} = q_h - u\beta_x \tag{3}$$

where

θ = Pipeline elevation

g = Gravitational constant

s = Specific entropy

a = Speed of sound

q_h = Net rate of heat flow from external sources to the fluid

β_x = Frictional force term

$$\psi = \left(\frac{\partial P}{\partial s}\right)_\rho \tag{4}$$

Briefly, the flow modeling involves the numerical solution of the mass, energy, and momentum conservation equations assuming (1-D) flow using a suitable technique such as the method of characteristics.[24] This involves the discretization of the pipeline into a sufficiently large number of space and time elements and determining the transient fluid properties such as pressure, temperature, density, and the fluid phase at the intersection of characteristics lines using interpolation, successive iteration, and flash calculations. Liquid and vapor phases are assumed to be at thermal and mechanical equilibrium. Heat transfer and frictional effects are determined using established flow- and phase-dependent correlations for hydrocarbon mixtures. The modeling of the complete depressurization of a pipeline typically involves several million calculations, thus, leading to the significant computational workloads synonymous with such simulations.

PipeTech's extensive validation against real pipeline rupture data is shown elsewhere (see for example[6,7]). For the sake of completeness, Figures 1 and 2, respectively, show the comparison of the simulated intact (curve A) and open end (curve B) pressure and temperature variations with time against the Isle of Grain pipeline rupture data.[19] Briefly, the tests involved depressurization of an instrumented 100-m long and 0.154 m inside diameter pipe containing commercial LPG (95% propane and 5% *n*-butane) at pressure and temperature of 21.6 bar and 17.8°C, respectively. As it may be observed, in all cases, PipeTech produces relatively good predictions of the test data. The initial rapid decline in pressure at the open end (Figure 1, curve C) is due to the transition of the liquid to the two-phase region. The eventual recovery in the open end fluid temperature (Figure 2, curve C) during the latter stages of the depressurization, on the other hand, is due to the warming of the fluid by the pipe wall. Figure 3 on the other hand shows the corresponding

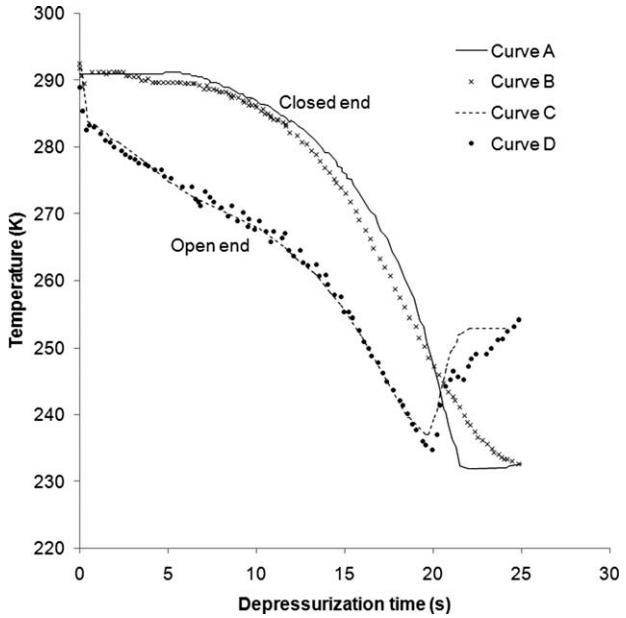

Figure 2. Temperature–time profiles at closed and open ends for the Isle of Grain P40 (LPG).

Curve A: field data (closed end); Curve B: PipeTech predictions (closed end); Curve C: field data (open end); Curve D: PipeTech predictions (open end).

pressure/time decay curves for two puncture diameters of 95 (Test P45) and 70.4 mm (Test P47). In the absence of a reported value, a discharge coefficient of 0.8 for gas/two-phase flows was used.

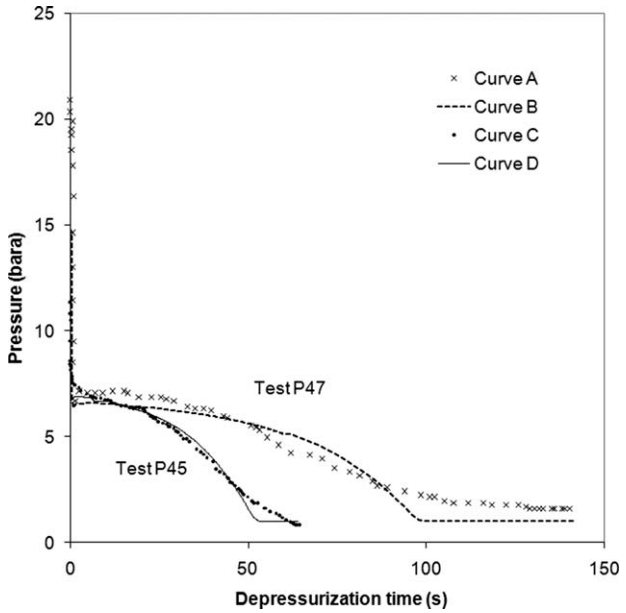

Figure 3. Pressure–time profiles for the Isle of Grain P45 and P47 tests (LPG).

Curve A: field data (Test P47); Curve B: PipeTech predictions (Test P47); Curve C: field data (Test P45); Curve D: PipeTech predictions (Test P45).

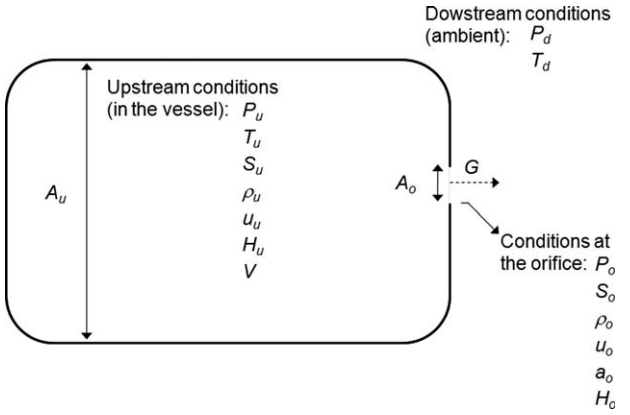

Figure 4. Schematic representation of the discharging vessel indicating the pertinent physical and thermodynamic properties required for the formulation of the outflow through the orifice using the VBM.

Vessel blowdown model

Figure 4 is a schematic representation of the discharging vessel indicating the pertinent physical and thermodynamic properties required for the formulation of the outflow through the orifice.

The corresponding energy conservation is given by[27]:

$$udu + gdz + dH - \delta q + \delta W_s = 0 \tag{5}$$

where u, g, z, and H, respectively, represent the mean fluid velocity, gravitational field constant, elevation, and the fluid enthalpy. q and W_s, on the other hand, represent the net heat flow into the system and shaft work, respectively.

Assuming horizontal flow, zero shaft work, and sufficiently high-flow rate through the orifice such that heat transfer between the flowing fluid and the orifice is negligible, Eq. 5 reduces to:

$$udu + dH = 0 \tag{6}$$

Furthermore, assuming that cross-sectional area (A_u) of the vessel is significantly larger than that for the orifice (A_o), the upstream fluid velocity relative to the downstream fluid velocity may be neglected. Integrating Eq. 6 from upstream to orifice conditions produces:

$$H_u = H_o + \frac{1}{2}u_o^2 \tag{7}$$

The fluid densities and phase equilibrium data at any given pressure and temperature are determined using the Peng–Robinson equation of state.[28] This equation has been shown to be particularly applicable to high-pressure hydrocarbon mixtures (see for example[29]). The number and the appropriate fluid phases present at any given temperature and pressure on the other hand are determined using the Gibbs tangent plane stability test.[30,32]

The following section describes the methodology employed for solving the energy balance Eq. 7 for permanent gas and two-phase mixtures.

Permanent gas

In the case of choked gas flow where no condensation takes place across the orifice, Eq. 7 is solved for u_o iteratively using the Brent iteration method.[33] In essence, the procedure involves an initial guess of the chocked pressure, P_o and updating it based on isentropic expansion across the orifice ($S_o = S_u$) until Eq. 7 is satisfied. Once the solution is obtained, other pertinent flow parameters such as density and temperature are determined using pressure-entropy flash calculations.

The fluid orifice velocity, u_o, under chocking conditions is equal to the speed of sound. The latter is determined from the analytical solution of the following equation based on the Peng–Robinson equation of state:

$$a^2 = \left(\frac{\partial P}{\partial \rho}\bigg|_S\right) \tag{8}$$

where a is the sonic velocity.

For subsonic gas flows, no iterations are required for determining the flow parameters at the orifice. Here, the orifice pressure, P_o is equal to the ambient pressure. Given that, $S_u = S_o$, the discharge parameters such as density, pressure, and enthalpy are simply obtained based on pressure/entropy flashes at P_o and S_o. The orifice discharge velocity u_o, is then determined from Eq. 7, because all the remaining parameters are known.

The variation of mass release rate with time is determined by approximating the depressurization process by a series of variable pressure reductions. The average mass flow rate between each pressure interval is then determined from u_o and ρ_o based on the procedure described above. The advantages of using pressure steps are in its thermodynamic convenience and computational efficiency when compared with choosing time intervals that are thermodynamically irrelevant.[20]

The time lapsed between the successive pressure intervals is determined from the mass loss from the vessel's fixed volume and dividing it by the average mass flow rate.

It should be noted that for simplicity, the expansion of the fluid within the vessel is assumed to be isothermal. This assumption holds provided the depressurization rate is sufficiently slow to allow perfect heat transfer between the expanding gas and the vessel's walls. The credibility of this assumption will be investigated later based on the comparison of the vessel with the pipeline outflow predictions.

Two-phase mixture

Assuming that no work is done by the fluid following its adiabatic expansion across the orifice, the energy balance produces:

$$dh_e = vdP \tag{9}$$

where, v is the fluid specific volume of the two-phase mixture. Substituting Eq. 9 into Eq. 6 and integrating produces:

$$\int_{Pu}^{Po} -vdP = \frac{1}{2}u_o^2 \tag{10}$$

Expressing Eq. 10 in terms of the mass flux:

$$G = \frac{\left[2\int_{Pu}^{Po} -vdP\right]^{1/2}}{v} \tag{11}$$

The solution of Eq. 11 first requires an appropriate equation of state expressing the specific volume of the two-phase mixture in terms of pressure and temperature coupled by an iterative procedure to determine the orifice pressure, P_o. As convergence using the above procedure proved impossible, the approximate ω-method[34,35] widely used for sizing of safety valves in the oil and gas industry is used in this study.

Given the significantly higher sensible heat of the condensed phase when compared with the vapor, the expansion across the orifice is considered as being isothermal. Furthermore, the vapor phase is assumed to follow ideal gas behavior. The orifice choke pressure, P_o, is obtained by solving the following equation using the bisection method[36]:

$$\eta^2 + (\omega^2 - 2\omega)(1-\eta)^2 + 2\omega^2 \ln\eta + 2\omega^2(1-\eta) = 0 \tag{12}$$

where

$$\eta = P_o/P_u \tag{13}$$

and

$$\omega = \frac{x_u v_{v,u}}{v_u} + \frac{C_{pl,u}T_u P_u}{v_u}\left(\frac{v_{vl,u}}{H_{vl,u}}\right)^2 \tag{14}$$

x and C_P are the vapor mass fraction and specific heat capacity at constant pressure, respectively. The subscripts, v and l on the other hand, respectively, refer to the vapor and liquid phases. Subscript, u denotes the upstream condition.

Once the choke pressure is known, in the absence of an analytical solution, the speed of sound for the two-phase mixture assumed to be fully dispersed is evaluated numerically[10] from:

$$a^2 = \left(\frac{\Delta P}{\rho(T,P) - \rho(T^*, P-\Delta P)}\right)_s \tag{15}$$

where the density of the two-phase mixture, with a vapor mass fraction, χ is calculated from:

$$\rho = \frac{\rho_v \rho_l}{\rho_v(1-\chi) + \rho_l \chi} \tag{16}$$

The incremental pressure step, ΔP in Eq. 15 is taken as 10^{-6} bar. The temperature, T^*, is obtained by minimizing the following function using Newton–Raphson's method[36]:

$$\omega^{(n)} = S(T,P) - S(T^{*(n)}, P-\Delta P) \tag{17}$$

where n denotes the iteration number.

For two-phase subsonic flow, the solution procedure for the discharge rate calculation is the same as that for the permanent gas described above.

Table 1. Pipeline Characteristics and Prevailing Conditions

Parameter	Value			
Pipe length, L (km)	0.1		1	5
Pipe inner diameter, D (mm)	300			
Pipe wall thickness (mm)	10			
Line pressure (bar)	21		50	100
Initial temperature (K)	300			
Ambient pressure (bar)	1.01			
Ambient temperature (K)	290			
Puncture location	Mid length			
Discharge coefficient	1			
Puncture diameter, d_o (mm)	30	60	90	120
Puncture to inner pipe diameter ratio (d_o/D)	0.1	0.2	0.3	0.4
Pipe wall material	Carbon steel			
Pipe wall density (kg/m^3)	7854			
Wind velocity (m/s)	0			
Pipe wall thermal conductivity (W/m^{2}K)	53.65			
Pipe roughness (mm)	0.05			

Results and Discussions

The following describes the results of a series of investigations aimed at establishing the range of applicability of the VBM for simulating pipeline punctures. This is based on comparing the VBM predictions against those obtained from the rigorous but computationally demanding numerically based PipeTech.

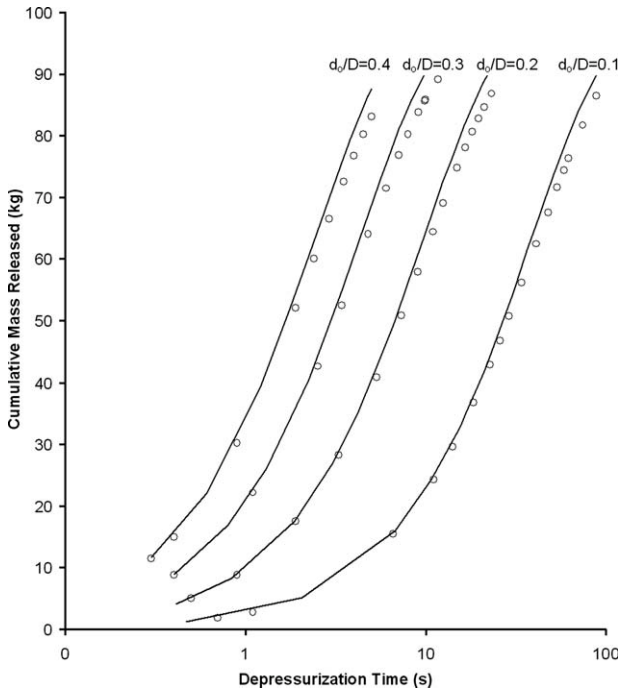

Figure 5. Comparison of cumulative mass released against time during depressurization to 1 bar based on VBM (solid line) and PipeTech (data points) for different puncture/pipe diameter ratios, do/D.

Inventory: 100% Methane; Initial pressure: 21 bar; Pipeline length: 100 m.

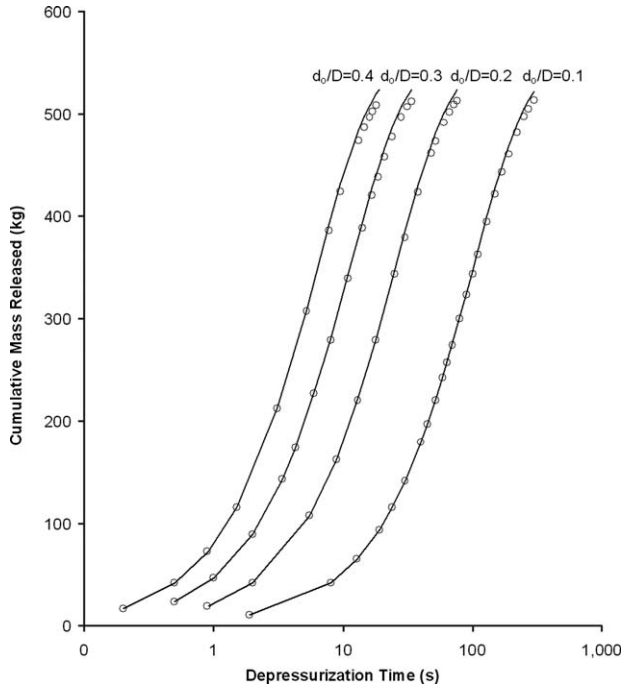

Figure 6. Comparison of cumulative mass released against time during depressurization to 1 bar based on VBM (solid line) and PipeTech (data points) for different puncture/pipe diameter ratios, do/D.

Inventory: 50% methane and 50% *n*-pentane; Initial pressure: 21 bar; Pipeline length: 100 m.

Table 1 shows the prevailing conditions, pipeline characteristics, and the range of parameters used in the proceeding investigations. The pipeline is assumed to be made of mild steel. Puncture/pipeline diameter ratios, d_o/D in the range 0.1–0.4 covering realistic failure scenarios, are considered. For the pipeline simulations, an automatic nested grid system[6] in which smaller time and distance discretization steps are used near the puncture plane to capture the rapid transients. For simplicity, a discharge coefficient of unity is assumed. All simulations are performed using a 2.66 GHz, 3.0-GB RAM PC. Pipeline failure is assumed to be in the form of a puncture midway along the uninsulted pipeline exposed to still air.

To allow direct comparison, the vessel is assumed to have the same volume and remain at the same initial conditions as the pipeline. Given that in the case of VBM, the bulk fluid expansion within the vessel is assumed to be isothermal, other remaining characteristics such as wall thickness, overall dimensions, shape, and heat-transfer coefficients are irrelevant.

Impact of the puncture/pipeline diameter ratio, d_o/D

Figures 5 and 6, respectively, show the predicted cumulative mass released against time following pipeline puncture at 21 bar based on the two discharge models for pure gaseous methane and an equimolar two-phase mixture of methane and *n*-pentane. The data are determined at different puncture/pipeline diameter ratios in the range 0.1–0.4 for a 100-m pipeline chosen as an example. At the prevailing

Table 2. Average Percentage Errors in the Cumulative Mass Released for VBM Predictions at Different Puncture to Pipe Diameter Ratios for the Permanent Gas (Methane) and the Two-Phase Mixture (Methane and *n*-Pentane)

	Average % error	
Puncture/pipe diameter ratio, d_o/D	Permanent gas (methane)	Two-component mixture (methane and *n*-pentane)
0.1	3.52	0.96
0.2	3.86	1.25
0.3	4.1	1.32
0.4	4.29	1.46

Initial pressure: 21 bar; Pipeline length: 100 m.

conditions tested (see Table 1), methane remains in the gaseous state throughout the depressurization to 1 bar. The solid lines represent the VBM data. The data points on the other hand are from PipeTech.

As it may be observed, in both cases the VBM produces generally good agreement with PipeTech predictions throughout. However, the degree of agreement reduces during the latter stages of depressurization where the VBM slightly over-predicts the cumulative mass released.

Table 2 presents the corresponding average errors in the VBM cumulative mass-released predictions based on comparison with PipeTech at different puncture/pipeline diameter ratios. As it may be observed, the percentage error in the VBM predictions increases with increase in the puncture/pipeline diameter. This is a consequence of the increasing inapplicability of negligible bulk fluid motion assumption in the vessel with the increase in the puncture diameter.

Also, surprisingly, the VBM model produces significantly smaller average errors in the case of the two-phase mixture when compared with the gaseous inventory.

To explain the above, Figures 7 and 8 show the axial variations in the fluids temperatures in the vicinity of the puncture at different time intervals up to 20 s following puncture. A puncture/pipeline diameter ratio of 0.2 is chosen as an example. Figure 7 is for gaseous methane, whereas Figure 8 presents the data for the two-phase methane/*n*-pentane mixture. The temperature profiles were generated using PipeTech, which takes into account phase-dependent transient heat-transfer effects.[8]

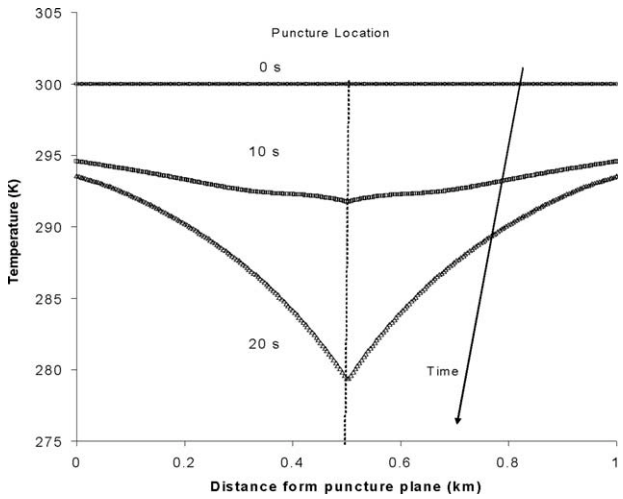

Figure 7. The variation of the fluid temperature profile in the vicinity of puncture at different time intervals following puncture for methane.

Puncture/pipe diameter ratio; 0.2; Pipeline length: 1000 m.

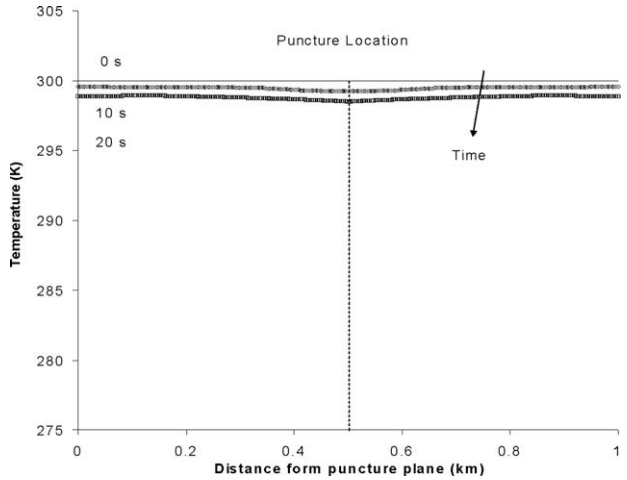

Figure 8. The variation of the fluid temperature profile in the vicinity of puncture at different time intervals following puncture for the two-phase methane–pentane mixture.

Puncture/pipe diameter ratio: 0.2; Pipeline length: 1000 m.

As it may be observed, in the case of the gaseous inventory (Figure 7), at any given time interval following puncture, the drop in the temperature due to its expansion-induced cooling is significantly higher than that for the two-phase mixture (Figure 8). At 20 s following puncture, for example, the maximum drop in the gas temperature is about 22°C. This compares with only 2°C for the two-phase mixture.

The higher depressurization-induced cooling of the gas is simply due to its larger Joule Thomson expansion coefficient when compared with the two-phase mixture.

Given that the VBM is based on the isothermal bulk fluid expansion assumption within the vessel, the above findings are consistent with its better performance in the case of the two-phase mixture when compared with the gaseous inventory.

Impact of the pipe length

Figures 9 and 10, respectively, show the cumulative mass released against depressurization time predictions based on VBM and PipeTech for different pipeline lengths in the range 100–5000 m for the gaseous and the two-phase mixture. The data are generated at the largest puncture/pipeline diameter ratio of 0.4.

Table 3 represents the corresponding average errors in the VBM cumulative mass-released predictions for both inventories at the different pipe lengths.

Once again, relatively good agreement between the two predictions is obtained for all the pipe lengths investigated. The largest average error in the VBM prediction corresponding to the shortest pipeline length (100 m) for the gaseous phase is 4.3%.

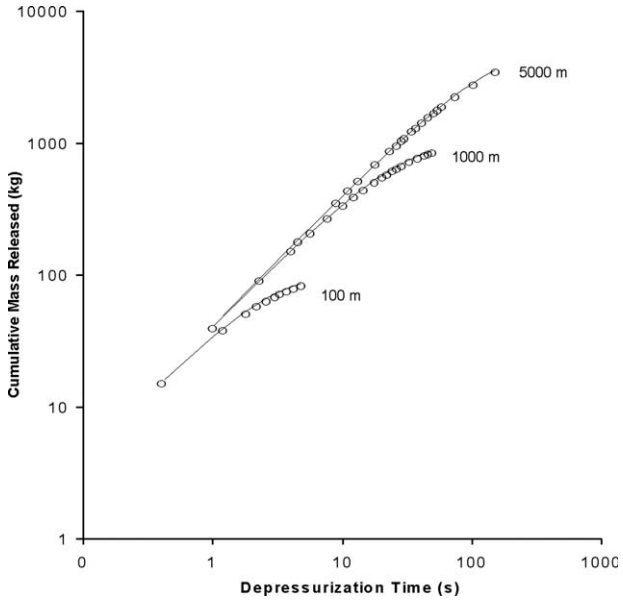

Figure 9. Comparison of the cumulative mass released against depressurization time to 1 bar for VBM (solid line) and PipeTech (data points) at different pipe lengths, L.

Inventory: methane; Puncture/pipe diameter ratio: 0.4; Initial pressure: 21 bar.

Much the same as with the decreasing diameter ratio, the VBM performs better as the pipeline length is increased. In the case of the puncture of a long isolated pipeline where there is no initial flow, given the large amount of inventory present, the impact of the localized

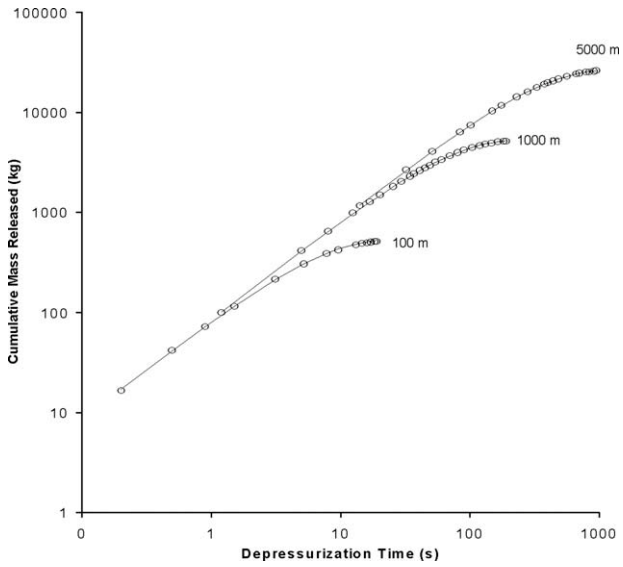

Figure 10. Comparison of the cumulative mass released against depressurization time to 1 bar for VBM (solid line) and PipeTech (data points) at different pipe lengths, L.

Inventory: 50% methane, 50% *n*-pentane; Puncture/pipe diameter ratio: 0.4; Initial pressure: 21 bar.

Table 3. Average Percentage Errors in the Cumulative Mass Released for the VBM Predictions at Different Pipeline Lengths

	Average % error	
Pipe length, L (m)	Permanent gas (methane)	Two-component mixture (methane and *n*-pentane)
100	4.30	1.46
1000	2.55	0.42
5000	1.61	0.35

Puncture to pipe diameter ratio: 0.4; Initial pressure: 21 bar.

expansion induced cooling effects in the bulk fluid on the outflow is less important when compared with that for shorter pipelines. As the VBM ignores such effects, its better performance with increase in the pipeline length is to be expected.

Also, once again, the VBM performs better for the two-phase inventory when compared with the gas, producing respective average errors of 4.3 and 1.46% for the 100-m pipe.

Impact of the line pressure

Figures 11 and 12 show the comparisons of cumulative mass released against depressurization time for different initial line pressures of 21, 50, and 100 bar based on VBM and PipeTech predictions. Figure 11 shows the data for gaseous methane, whereas Figure 12 shows the corresponding data for and the two-phase methane/*n*-pentane mixture. The pipe length and diameter ratio chosen are 100 and 0.4 m, respectively, representing the worse conditions in terms of the

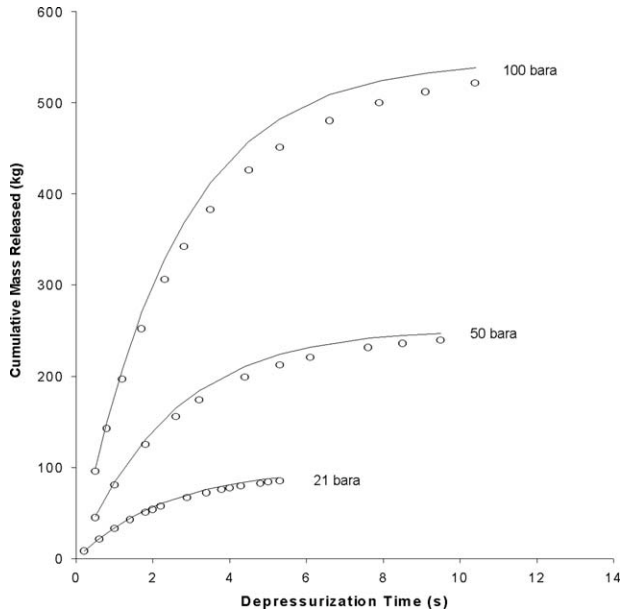

Figure 11. Comparison of the cumulative mass released against depressurization time to 1 bar based on VBM (solid line) and PipeTech (data points) predictions for different initial line pressures.

Inventory: 100% Methane; Puncture/pipe diameter ratio: 0.4; Pipeline length: 100 m.

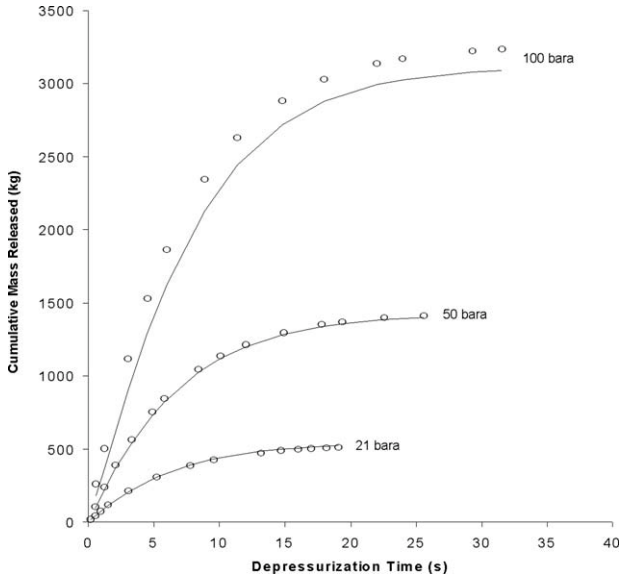

Figure 12. Comparison of the cumulative mass released against depressurization time to 1 bar based on VBM (solid line) and PipeTech (data points) predictions for different initial line pressures.

Inventory: 50% methane, 50% *n*-pentane; Puncture/pipe diameter ratio: 0.4; Pipe length: 100 m.

applicability of the VBM. In line with the previous findings, in the case of gaseous methane, the VBM produces higher predictions of the cumulative mass released when compared with the PipeTech. Also, VBM's performance deteriorates with increase in the starting line pressure and depressurization time. The former is due to the inapplicability of the permanent gas behavior assumption at high pressures. Also, the isothermal bulk gas assumption becomes less relevant as the pipeline depressurizes.

In the case of the two-phase mixture, however (Figure 12), very good agreement between the two models may be observed at all the conditions tested with the exception of 100 bar line pressure where the VBM underpredicts the cumulative mass released throughout the depressurization. Further investigations reveal that this is due to failure of Eq. 12 in predicting the correct chocked pressure. This results in underprediction of the discharge rate and hence the cumulative mass released.

Table 4 presents the corresponding average errors in the VBM cumulative mass-released predictions at the different initial line pressures for gaseous methane and the two-phase methane/*n*-pentane mixture. As before, with the exception of 100 bar, the VBM performs better in the case of the two-phase mixture when compared with the gaseous inventory.

Table 4. Average Percentage Errors in the Cumulative Mass Released based on the VBM Predictions at Different Initial Line Pressures

Initial line pressure (bar)	Average % error	
	Permanent gas (methane)	Two-component mixture (methane and *n*-pentane)
21	4.30	1.46
50	4.60	2.47
100	5.77	11.44

Puncture to pipe diameter ratio: 0.4; Pipe length: 100 m.

Table 5. Computational Runtimes for VBM and PipeTech models

Inventory	Pipe length (m)	Computational run time	
		PipeTech	VBM (s)
Methane	100	4 min, 2 s	0.321 s
	1000	35 min, 2 s	0.322 s
	5000	4 h, 12 min, 33 s	0.320 s
50% Methane and 50% *n*-pentane	100	2 h, 15 min, 5 s	1.022 s
	1000	5 h, 34 min, 33 s	1.022 s
	5000	12 h, 18 min, 33 s	1.019 s

Initial pressure: 21 bar. Puncture to pipe diameter ratio: 0.2.

Computational run-time

Table 5 presents the computational run times for different pipe lengths based on VBM and PipeTech for the permanent gas and the two-phase mixture puncture simulations. For the sake of an example, the selected line pressure and diameter ratio are 21 and 0.4 bar, respectively.

As it may be observed, given that the VBM solution method is primarily analytically based, the corresponding computational run times in all the cases presented are orders of magnitude smaller than those based on the PipeTech. Such reductions are especially marked for the two-phase mixture. For the 5000-m pipeline, for example, the VBM computational run time is about 12 h when compared with only about 1 s for the PipeTech. In this case, approximating the punctured pipe as a vessel results in an average error of only 0.35% (see Table 3).

Conclusions

This article investigated the tantalizing important question of if and under what conditions the outflow from a punctured pipe can be modeled as that discharging from a vessel. Given that the latter may be solved analytically, this study addresses the fundamentally important drawback of the long computational run times associated with the numerical techniques for simulating pipeline punctures.

The investigations involved the development and application of a simplified VBM and comparing its predictions against a rigorous but computationally demanding pipeline rupture model, PipeTech for a variety of test conditions. These included variations in the pipe length, puncture/pipeline diameter ratio, and line pressure for both a permanent gas and a two-phase mixture. The results indicated that in the majority of cases, relatively good agreement between the two methods of solution was obtained. The degree of agreement was found to increase with decrease in the diameter ratio and line pressure. An increase in the pipe length also improved the degree of agreement.

In essence, the VBM performs well in predicting outflow from a punctured pipeline for as long as there is negligible relative bulk flow between the discharging fluid and the pipe wall. This study identified the conditions for departure from this flow regime.

Surprisingly, the VBM performed better in the case of the two-phase inventory when compared with the permanent gas. An investigation of the fluid temperature profiles in the proximity of the puncture showed that this was due to the better applicability of the VBM isothermal bulk fluid expansion assumption in the case of the two-phase mixture as compared to the gas.

The PipeTech computational workload in the case of the two-phase mixture was found to be significantly higher than that for the gas. This makes the application of the VBM for simulating the puncture of pressurized pipelines containing two-phase mixtures particularly attractive.

It should be noted that the above investigations were conducted for an isolated pipeline. A useful extension of this study would be extending the VBM to account for the effect of feed flow from a pump during puncture.

Of course, the VBM is wholly inapplicable for the most catastrophic type of pipeline failure involving full bore or guillotine ruptures. The development of an analytical solution technique for modeling such failures is considered as the Holy Grail by the pipeline modelers.

Literature Cited

1. List of Pipeline Accidents. Available at: http://en.wikipedia.org/wiki/List_of_pipeline_accidents. Updated March 19, 2010. Accessed September 17, 2010.
2. US Department of Transportation—Office of Pipeline Safety. Available at: http://primis.phmsa.dot.gov/comm/reports/safety/PSI.html. Updated March 9, 2010. Accessed September 17, 2010.
3. Mahgerefteh H, Atti O. Modeling low-temperature-induced failure of pressurized pipelines. *AIChE J*. 2006;52:1248–1256.
4. Bilio M, Brown S, Fairweather M, Mahgerefteh H. CO_2 pipelines material and safety considerations. HAZARDS XXI Process Safety and Environmental Protection. *IChemE Symp Ser*. 2009;155:423–429.
5. Connolly S, Cusco L. Hazards from high pressure carbon dioxide releases. HAZARDS XX Process Safety and Environmental Protection. *IChemE Symp Ser*. 2007;153:237–242.
6. Mahgerefteh H, Saha P, Economou IG. Fast numerical simulation for full bore rupture of pressurised pipelines. *AIChE J*. 1999;45:1191–1201.
7. Oke A, Mahgerefteh H, Economou IG, Rykov Y. A transient outflow model for pipeline puncture. *Chem Eng Sci*. 2003;58:4591–4604.
8. Mahgerefteh H, Oke A, Atti O. Modelling outflow following rupture in pipeline networks. *Chem Eng Sci*. 2006;61:1811–1818.
9. Mahgerefteh H, Oke A, Rykov Y. Efficient numerical simulation for transient flows. *Chem Eng Sci*. 2006;61:5049–5056.
10. Mahgerefteh H, Atti O, Denton G. An interpolation technique for the rapid CFD simulation of highly transient flows. Process Safety & Environmental Protection. *Trans IChemE B*. 2006;84(B6):1–6.
11. Chen JR, Richardson SM, Saville G. Modelling of two-phase blowdown from pipelines—I A hyperbolic model based on variational principles. *Chem Eng Sci*. 1995;59:695–713.
12. Chen JR, Richardson SM, Saville G. Modelling of two-phase blowdown from pipelines—II A simplified numerical method for multicomponent mixtures. *Chem Eng Sci*. 1995;59:2173–2187.
13. Bendiksen KH, Malnes D, Moe R, Nuland S. The dynamic two-fluid model OLGA theory and application. *SPE Production Eng*. 1991;6:171–180.
14. Hall ARW, Butcher ER, Teh CE. Transient simulation of two-phase hydrocarbon flows in pipelines. Proceedings of the European Two-Phase Flow Group Meeting. Hannover, 1993:73–82.
15. Nordsveen M, Haerdig A. Simulations of severe slugging during depressurisation of an oil/gas pipeline. Proceedings of SIMS Simulation Conference. Trondheim, 1997;18:61–73.
16. Peterson CE, Chexal VK, Clements TB. Analysis of a hot-leg small break LOCA in a three loop Westinghouse PWR plant. *Nuc Tech*. 1985;70:104–109.
17. Shoup G, Xiao JJ, Romma JO. Multiphase pipeline blowdown simulation and comparison to field data. BHR Group Conference Series No. 31. 1998:171–179.
18. Geurst JA. Variational principles and two-fluid hydrodynamics of bubbly liquid/gas mixtures. *Physica A*. 1986;135:455–486.
19. Richardson SM, Saville G. Blowdown of LPG pipelines. *Trans Inst Chem Eng B*. 1996;74:235–244.
20. Mahgerefteh H, Wong SMA. A numerical blowdown simulation incorporating cubic equations of state. *Comput Chem Eng*. 1999;23:1309–1317.
21. Norris HL, III. Single-phase or multiphase blowdown of vessels or pipelines. *Society of Petroleum Engineers [SPE 26565]* 1993:519–528.
22. Norris HL, III. Hydrocarbon blowdown from vessels and pipelines. *Society of Petroleum Engineers [SPE 28519]*. 1994:593–602.
23. Kelbaliev RF, Aliev RY, Ismailov MB. Heat transfer in a horizontal coiled pipe in a transient regime and at a near-critical pressure of a fluid. *J Eng Phys Thermophys*. 2008;81:930–934.
24. Zucrow MJ, Hoffman JD. *Gas Dynamics*, *Vol*. I and II. Wiley: New York, 1976.
25. PipeTech Pipeline Rupture Computational Fluid Dynamics Simulator. Available at: http://www.pipetechsoftware.com. Update August 25, 2010. Accessed September 17, 2010.
26. Mahgerefteh H, Saha P, Economou IG. Modelling fluid phase transition effects on the dynamic behaviour of ESDV. *AIChE J*. 2000;46:997–1006.
27. Backhurst JR, Coulson JM, Harker JH, Richardson JF. *Chemical Engineering Volume 1: Fluid Flow Heat Transfer and Mass Transfer*, 6th Ed. London: Butterworth-Heinemann, 1999.
28. Peng DY, Robinson DB. A new two-constant equation of state. *Ind. Eng. Chem. Fundamen*. 1976;15:59–63.
29. Assael MJ, Trusler JPM, Tsolakis TF. *Thermophysical Properties of Fluids*. London: Imperial College Press; 1996.
30. Michelsen ML. The isothermal flash problem: I Stability. *Fluid Phase Equil*. 1982;9:1–19.
31. Michelsen ML. The isothermal flash problem: II Phase-split calculation. *Fluid Phase Equil*. 1982;9:21–40.
32. Michelsen ML. Multiphase isentalpic and isentropic flash algorithms. *Fluid Phase Equil*. 1987;33:13–27.
33. Press WH, Teukolsky SA, Vetterling WT, Flannery BP. *Numerical recipes in FORTRAN 77: The art of scientific computing*, 2nd ed. Cambridge: Cambridge University, 1992.
34. Leung JC, Grolmes MA. A generalized correlation for flashing choked flow of initially subcooled liquid. *AIChE J*. 1988;34:688–691.
35. Leung JC. Similarity between flashing and non-flashing two-phase flows. *AIChE J*. 1990;36:797–800.
36. Dahlquist G, Björck A. *Numerical Methods*. Englewood Cliffs, NJ: Prentice Hall, 1974.

Manuscript received Apr. 28, 2010, revision received Sept. 21, 2010, and final revision received Dec. 21, 2010.